Analysis of Mixed Convection Flow on Arrhenius-Controlled Heat Generating/Absorbing Fluid in a Super-Hydrophobic Microchannel: A Semi-Analytical Approach

Godwin Ojemeri[1]* and Isaac O. Onwubuya [2]

[1]Department of Mathematics,
College of Sciences,
Federal University of Agriculture,
P. M. B. 28, Zuru,
Kebbi State.

[2]Department of Mathematics, Faculty of Sciences,
Air Force Institute of Technology,
P. M. B. 2104,
Kaduna State.

Email: godwinojemeri@gmail.com

Abstract

The theoretical analysis of steady mixed convection with Arrhenius-controlled heat flow for a viscous and an electrically-conducting fluid traveling across an isothermally heated vertical parallel plate in a slit micro-channel is investigated in this study. One wall had super-hydrophobic slip and a temperature spike, while the other did not. A semi-analytical technique (perturbation series) was employed to analyze the nonlinear and coupled leading equations. The results were carefully scrutinized, and the effects of the relevant and pertinent parameters were illustrated using various plots. It is concluded from this work that the actions of mixed convection and chemically reacting factors are noticed to substantially strengthen the fluid movement in the micro-channel for a constant pressure gradient. Additionally, the function of heat source parameter is depicted to raise the fluid flow while heat absorption parameter yields the reverse phenomenon. In the fields of engineering and medicine, it is essential to understand these fluids' characteristics. Owing to the lubrication of micro-channel boundary surfaces where conductivity and viscosity interact with thermos-physical behavior, the results of the present investigation can significantly enhance the functioning of micro-electro-mechanical systems (MEMS) and micro-devices relying on micro-fabrication processes.

Keywords: Mixed convection, Arrhenius-controlled fluid, super-hydrophobic slip, temperature jump, heat generating/absorbing effect.

Nomenclature

B_0 =constant magnetic flux density [kg/s^2.m^2]

g=gravitational force [m/s^2]

h= channel size [m]

C_pC_v=specific heats at constant pressure and constant volume [Jkg^{-1}K^{-1}]

M= magnetic field

e=activation energy

$\frac{Gr}{Re} = Gre$=Mixed convection parameter

$\frac{dP}{dX} = A$= pressure gradient

Author for Correspondence

S= heat generating/absorbing parameter
Nu=dimensionless heat transfer rate
T=dimensionless temperature of the fluid [K]
T_0=reference temperature [K]
u=dimensionless velocity of the fluid [ms^{-1}]
y= dimensionless distance between plates
U_0=reference velocity [ms^{-1}]

Greek letters
γ =dimensionless slip length parameter
Γ =dimensionless temperature jump parameter
λ =chemical reacting parameter
β =thermal expansion coefficient [K^{-1}]

$\beta_t \beta_v$ =dimensionless variables
μ =variable fluid viscosity [kgm^{-1}s^{-1}]
k=thermal conductivity [m.kg/s^3.K]
α =thermal diffusivity [m^{2}s^{-1}]
γ_s = ratios of specific heats ($C_p C_v$)
σ =conductivity of the electric fluid [s^{3}m^2/kg]
ρ = fluid density[kgm^{-3}]
v =viscosity of the fluid [m^{2}s^{-1}]

Introduction
The enormous advancement of technology in response to people's demand for smaller machines and lighter devices has propelled the scientific community, engineers, and innovators' attention to exploration, simulation, and theoretical investigations in mini-technology, then micro-technology, and finally nano-technology. This is what motivated scholars in computational fluid dynamics to divert their focus from analyzing flows in macro-channels to investigating flows in mini-channels, micro-channels, and nano-channels. Micro-channel fluid and thermal transport flows have grown tremendously in recent times as a result of their diverse significance in material processing activities and fabrication; micro energy pipes; space technology; micro-channel internal heat generation; micro-jet boundary layer cooling; large power density transistors in high-performance computing; and other devices. Since most of these formulations involve inner micro-channel flows, comprehending the flow characteristics has become extremely crucial for proper and appropriate simulation projections and conceptualization (Al-Nimr and Khadrawi 2004; Jha *et al.* 2014a).

Numerous studies have been published on the role of the flow regime on micro-structure in a range of physical situations. In light of the foregoing, Hamza *et al.* (2023) recently investigated a theoretical study on the impact of Arrhenius-controlled heat transfer flow influenced by an induced magnetic field in a microchannel. Ojemeri and Hamza (2022) proposed an analysis of Arrhenius kinetically provoked heat source/sink fluid in a microchannel using the homotopy perturbation technique. Jha and Malgwi (2019a) outlined the implications of Hall current and ion-slip on hydro-magnetic heat transfer flow in a vertical micro-channel affected by an applied magnetic field. The modeling of MHD convection in an upstanding micro-channel composed of two electrically non-conducting unlimited vertical parallel plates was carried out by Jha and Aina (2016). Jha *et al.* (2017) discussed the consequence of Hall current on hydro-magnetic natural convection in a vertical microchannel

as part of their investigation. Some other research conducted on this area include (Chen and Weng 2005; Buonomo and Manca, 2012; Weng and Chen 2009; Jha *et al.* 2015; Jha *et al.* 2014b), to highlight a few.

Magneto hydrodynamic (MHD) analysis has grown in popularity in recent decades as a result of the concept's usefulness in a variety of MHD functions, including MHD generators, cooling baths with cooling metallic plates, electric transformers, and MHD injectors. Chemical energy technology, which includes the use of MHD pumps to transfer electrically conductive fluids, is currently employed in some nuclear power plants. In addition to these purposes, when the fluid is electrically conductive, an applied magnetic field can significantly boost free convection flow (Jha *et al.* 2015). Several studies on hydro-magnetic convective flow have been executed under a variety of natural conditions. Ojemeri et al. (2023) recently investigated the MHD-free flow of an electrically conductive Casson fluid driven by heat radiation effect in a vertical porous channel. The perturbation approach was utilized by Taid and Ahmed (2022) to address the effects of the Soret effect, thermal dissipation, and chemical reaction on steady two-dimensional hydro-magnetic free convection along an inclined porous plate covered with porous media. Siva *et al.* (2021) worked on a heat transfer investigation of electroosmotic flow in a rotating microfluidic channel and demonstrated a precise response to the MHD action. When Joseph *et al.* (2015) analyzed the unsteady MHD poiseuille flow through two infinitely parallel porous plates in an inclined magnetic field, they also took heat and mass transport into account. They found out that as the Hartman number Ha increases, so does the rate at which it moves. The thermal Grashof number Gr and the solutal Grashof number Gc increase velocity. Geethan *et al.* (2016) discussed the actions of thermal radiation, chemical reactions, and soret on MHD free convection slip flow down an inclined plate at a constant temperature affected by the heat source. Sivaiah and Reddy (2017) conducted a theoretical study of MHD free convective mass and energy transfer fluid with thermal diffusion in the coexistence of Hall current and radiation effects.

Scientists, technologists, and engineers are paying much attention to the evaluation of the result of the new combination using hydro-magnetic natural convection in a super-hydrophobic (SHO) micro-channel. Oil and gas companies, semiconductor manufacturing facilities, and companies that assemble small equipment SHO surfaces have the ability to reduce drag in a flow because of the enormous slip obtained from liquid/solid interfaces, making it a particularly relevant parameter to gauge the extent of drag reduction depending on the slip length. In view of these considerations, a theoretical investigation of a natural hydro magnetic flow in a vertical slit micro-channel having super-hydrophobic slip and temperature jump was conducted by Jha and Gwandu (2017). Their research showed that the greatest upward velocity obtained by heating the super-hydrophobic wall is less than that recorded by heating the no-slip surface whenever there is a temperature leap and no super-hydrophobic slip, or both. The maximum velocities are equivalent when neither is present. Later, Jha and Gwandu (2019) investigated free convection of an electrically conducting fluid in an upstanding micro-channel having super-hydrophobic slip and temperature jump using non-linear Boussinesq approximation methods. Raising the temperature jump coefficient, according to the computational results, contributes to a decrease in temperature when the super-hydrophobic surface is heated and increases the temperature when the no-slip surface is heated. Later, Jha and Gwandu (2020) built on their previous work Jha and Gwandu (2017) by proposing an analytical investigation of free convection airflow across porous plates heated alternately, one channel with no slip and the other super-hydrophobic. Ramanuja *et al.* (2020) explored free convection in an isothermally heated channel with super-hydrophobic slip on one surface and a temperature rise, but no slip on the opposite side. Hatte and

Pitchumani (2021) used a fractional rough surface characterization to thoroughly and explicitly describe the impact of heat transfer flow within a cylinder with non-wetting surfaces. The approach examines the dynamic stability of the fluid interaction in the asperities of air-infused super-hydrophobic surfaces. Their findings show that, contrary to prevalent belief, super-hydrophobicity, defined by the largest contact angles, does not always result in peak convective heat transfer behavior and that, under specific fluid flow conditions, hydrophobic surfaces can provide excellent thermal performance.

The impact of Arrhenius-controlled fluid on micro-channels with super-hydrophobic (SHO) surfaces in the coexistence of mixed convection and internal heat source/sink have not been investigated in any of the above-mentioned literature, hence the motivation for this research. As a result, the focus of this paper is to present a theoretical investigation of a steady mixed convection of chemically reacting fluid in a vertical slit micro-channel with SHO surface influenced by heat source/sink. The perturbation procedure is employed to analyze the dimensionless nonlinear and coupled leading equations. The results of this study could be very helpful in areas such as in micro-devices made with micro-fabrication processes, in micro-electro-mechanical systems (MEMS), in the lubrication industry, in biomedical sciences, in the processing and extraction industries, to mention a few.

Mathematical formulation of the flow system

Imagine the steady, fully developed mixed convection flow of an electrically conducting fluid flowing steadily upward along an upstanding parallel plate micro-channel affected by Arrhenius kinetic and a heat source/sink. Due to a specific micro-engineering process, one of the surfaces is extremely tough to wet (super-hydrophobic). The other side (slip-resistant surface) was not tempered with either. As demonstrated in Figure 1, the super-hydrophobic surface is maintained at $y_0 = 0$ while the non-slip surface is maintained at $y_0 = L$. Since the super-hydrophilicity of a surface is more important than how it flows, different temperature jumps and slip conditions were used on the various plates. Following Jha and Gwandu (2017), the leading equations for the current problem are as follows, applying the usual Boussinesq buoyancy approximation with boundary conditions and assuming that the fluid is viscous, heat generating/absorbing and chemically reactive.
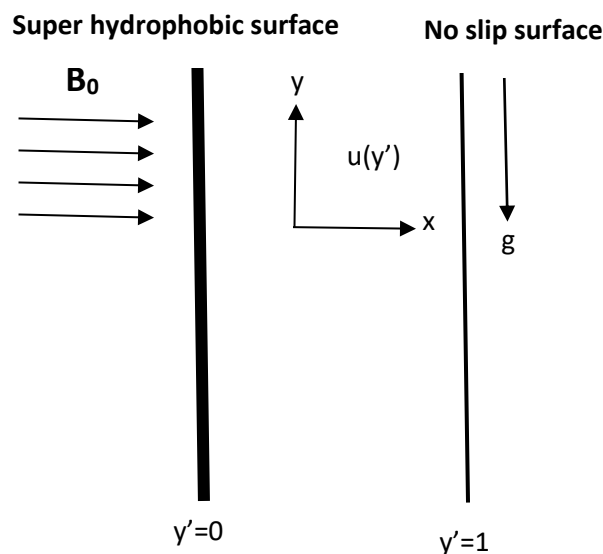

Figure 1 The schematic diagram of the flow

$$\frac{d^2U}{dy^2} + \frac{Gr}{Re}\theta - Ha^2U = A \tag{1}$$

$$\frac{d^2\theta}{dy^2} + \lambda e^{\frac{\theta}{1+\varepsilon\theta}} - S\theta = 0 \tag{2}$$

The boundary conditions in dimensionless forms are:

$$\theta(y) = 1 + \Gamma\frac{d\theta}{dy}, \qquad at\ y = 0 \tag{3}$$

$$u(y) = \gamma\frac{du}{dy}, \qquad at\ y = 0$$

$$\theta(y) = 0 \qquad at\ y = 1$$

$$u(y) = 0 \qquad at\ y = 1$$

The dimensional quantities used in deriving Equations 1-3 are as follows:

$$u = \frac{u'}{U}, y = \frac{y'}{h}, \theta = \frac{T'-T_0}{T_w-T_o}, x = \frac{x'v}{Uh^2}, \quad (Y,\gamma,\Gamma) = \frac{Y',\gamma',\Gamma'}{h}, Ha^2 = \frac{\sigma\beta_0^2h^2}{\rho v}$$

$$S = \frac{Q_0h^2}{k}, \ Re = \frac{U_0x}{v}, \ Gr = \frac{g\beta(T_w-T_0)h^3}{v^2}, A = -\frac{dP}{dx}, \lambda = \frac{QC_0^8AEH^2}{RT_0^2}, \varepsilon = \frac{RT_0}{E}$$

Where λ is the chemical reactant parameter, $\frac{Gr}{Re} = Gre$ is the mixed convection, $\frac{dP}{dX} = A$ is the pressure gradient, S is the heat generating/absorbing parameter, Γ is the temperature jump parameter, γ is the velocity slip parameter and Ha is the magnetic field intensity

Method of Solution

The momentum and energy equations can be reduced to the set of ordinary differential equations, which are solved semi-analytically by perturbation method.

we assume $\begin{array}{l}\theta = \theta_o + \lambda\theta_1 \\ U = U_o + \lambda U_1\end{array}\Big\}$ (4)

Substituting equation (4) into equations (1), (2) and (3) and taking the coefficient of λ^0 and λ, the following are the derived sets of ordinary differential equations and accompanying boundary conditions for temperature and velocity:

$$\lambda^0 : \frac{d^2U_o}{dy^2} + \theta_o - \frac{Gr}{Re}Ha^2U_o = A \tag{5}$$

$$\lambda : \frac{d^2U_1}{dy^2} + \theta_1 - \frac{Gr}{Re}Ha^2U_1 = 0 \tag{6}$$

$$\lambda^0 : \frac{d^2\theta_o}{dy^2} - S\theta_o$$
$$= 0 \tag{7}$$

$$\lambda : \frac{d^2\theta_1}{dy^2} - S\theta_1 = -1 - \theta_o - (2-e)\theta_0^2 \tag{8}$$

The boundary conditions at the both walls now become

$$\begin{array}{l}U_o = \gamma\frac{dU_o}{dy} \\ U_1 = \gamma\frac{dU_1}{dy}\end{array}\Big\}\ at\ y = 0$$

$$\begin{array}{l}U_o = 0 \\ U_1 = 0\end{array}\Big\}\ at\ y = 1 \tag{9}$$

and

$$\left.\begin{array}{r}\theta_o = 1 + \Gamma\dfrac{d\theta_o}{dy} \\ \theta_1 = \Gamma\dfrac{d\theta_1}{dy}\end{array}\right\} at \; y = 0 \\ \left.\begin{array}{r}\theta_o = 0 \\ \theta_1 = 0\end{array}\right\} at \; y = 1$$

(10)

The solution for temperature gradient is obtained as follows:

$$\theta_o = K_1 \cosh(y\sqrt{S}) + K_2 \sinh(y\sqrt{S}) \tag{11}$$

$$\theta_1 = K_3 \cosh(y\sqrt{S}) + K_4 \sinh(y\sqrt{S}) + F_1 + F_2 cosh(y\sqrt{S}) + F_3 sinh(y\sqrt{S})$$
$$+ F_4 cosh^2(y\sqrt{S}) + F_5 cosh(y\sqrt{S})sinh(y\sqrt{S}) + F_6 sinh^2(y\sqrt{S}) \tag{12}$$

The solution for velocity gradient is also obtained as follows:

$$U_0 = Q_1 \cosh(Hay) + Q_2 \sinh(Hay) \tag{13}$$

$$U_1 = Q_3 \cosh(Hay) + Q_4 \sinh(Hay) + \frac{Gr}{Re}(E_3 + E_1 cosh(y\sqrt{S}) + E_2 sinh(y\sqrt{S})$$
$$+ E_4 cosh^2(y\sqrt{S}) + E_5 cosh(y\sqrt{S})sinh(y\sqrt{S}) + E_6 sinh^2(y\sqrt{S})) \tag{14}$$

Recall that the expressions for temperature and velocity distributions are represented as follows:

$$\theta = \theta_0 + \lambda\theta_1 \quad\quad and \quad\quad U = U_0 + \lambda U_1$$

The rates of heat transfer and skin frictions at both micro-channel walls are obtained as follows:

$$\frac{d\theta}{dy}\Big|_{y=0} = K_2\sqrt{S} + \lambda[K_2\sqrt{S} + F_3\sqrt{S} + F_5\sqrt{S}] \tag{15}$$

$$\frac{d\theta}{dy}\Big|_{y=1} = K_1\sqrt{S}\sinh(\sqrt{S}) + K_2\sqrt{S}\cosh(\sqrt{S}) + \lambda[K_3\sqrt{S}\sinh(\sqrt{S}) + K_4\sqrt{S}\cosh(\sqrt{S}) +$$
$$F_2\sqrt{S}sinh(\sqrt{S}) + F_3\sqrt{S}cosh(\sqrt{S}) + 2\sqrt{S}F_4 cosh(\sqrt{S})sinh(\sqrt{S}) + F_5\sqrt{S}(sinh^2(\sqrt{S}) +$$
$$cosh^2(\sqrt{S})) + 2\sqrt{S}F_6 cosh(\sqrt{S})sinh(\sqrt{S})] \tag{16}$$

$$\frac{dU}{dy}\Big|_{y=0} = Q_2 Ha + \lambda\left[Q_4 Ha + \frac{Gr}{Re}E_2\sqrt{S} + \frac{Gr}{Re}E_5\sqrt{S}\right]$$

$$\frac{dU}{dy}\Big|_{y=1} = Q_1 Ha\sinh(Ha) + Q_2 Ha\cosh(Ha) + \lambda\Big[Q_3 Ha\sinh(Ha) + Q_4 Ha\cosh(Ha) +$$
$$\frac{Gr}{Re}E_1\sqrt{S}sinh(\sqrt{S}) + \frac{Gr}{Re}E_2\sqrt{S}cosh(\sqrt{S}) + 2\frac{Gr}{Re}\sqrt{S}E_4 cosh(\sqrt{S})sinh(\sqrt{S}) + \frac{Gr}{Re}E_5\sqrt{S}(sinh^2(\sqrt{S}) +$$
$$cosh^2(\sqrt{S})) + 2\frac{Gr}{Re}\sqrt{S}E_6 cosh(\sqrt{S})sinh(\sqrt{S})\Big] \tag{17}$$

Validation of results

The work of Jha and Gwandu (2017) is recovered successfully as λ, S and A approach 0 respectively, and setting $\frac{Gr}{Re}$ to be 1, thereby confirming an excellent agreement between this current research and their work. Table 1 showcases the numerical comparison between the work of Jha and Gwandu (2017) and the present work.

Results and discussion

The examination of Arrhenius-controlled heat source/sink fluid is performed on a fully developed mixed MHD flow of an electrically-conducting fluid passing through an isothermally heated parallel plate micro-channel, with one surface having SHS and temperature jump and the other having no slip. The regular perturbation series procedure is employed to determine the steady state equations. Various graphs were sketched to illustrate the functions of pertinent parameter namely chemically reacting parameter,λ, heat generation

parameter, S < 0, heat absorption parameter, S > 0 and magnetic field effect M on the fluid velocity and temperature gradient. The default values chosen for this investigation are (γ = Γ= 1, Ha=0.5, λ = 0.001, S=0.5, Gre = 10), except otherwise stated, as it relates to real life situation. Throughout this discussion, S < 0 and S > 0 will indicate heat generation and heat absorption respectively.

Figures 2a and b illustrate the function of heat source/sink factors on the temperature profile for fixed (γ = Γ= 1) values. Figure 2a depicts a surge in temperature for S < 0, while Figure 2b depicts a reduction in temperature for S > 0. Greater thermal gradients are anticipated as a result of heat emission parameters along the cold wall. This is the case since once heat has been absorbed, the fluid gets heavier and the convection current diminishes, leading to a decrease in the thermal fluid. In contrast, a rise in heat output makes the convection current stronger, which makes the fluid less dense and raises its temperature.

The actions of chemical reaction on the temperature profile are showcased in Figure 3. Clearly, as the value of λ improves, the temperature jumps significantly. According to Hamza (2016), raising the levels of λ, the temperature equation's viscous heating and chemical reactant factors are strengthened remarkably, causing a considerable temperature increase.

The consequences of increasing the heat generation and absorption values on the velocity gradient are plotted in Figures 4a and b. As the heat source (S< 0) and heat sink (S > 0) levels grow, the same effects that were observed in the energy gradient are replicated in the velocity gradient as expected. Naturally, this can be believed to be due to the added heat boost, which enhances the system's ability to transfer heat. This raises the temperature of the fluid and enhances flow in the system as a whole. Additionally, it is believed that the heat source/sink parameter close to the plate contains more heat, allowing the fluid to move more quickly and so expand the fluid's velocity and temperature within the boundary layer vicinity. Again, if the internal heat generation/absorption parameter is made bigger, the temperature and velocity boundary surfaces in the micro-channel get thicker.

Figure 5 plots the outlook of velocity for the deviations of mixed convection parameter. It can be seen that uplifting the level of the mixed convection parameter, the fluid velocity is drastically enhanced in the microchannel.

The function of λ on fluid velocity is demonstrated in Figure 6. It was evident that as λ mounts, an escalation in the fluid velocity was noticed. Also, it was shown that the fluid wall effect decreases as velocity slip rises at super-hydrophobic walls. This makes the gas move faster near the wall. A decline in fluid viscosity and a subsequent rise in fluid velocity are caused by the remarkable increase in temperature in reaction to the higher λ.

The effect of MHD on the velocity variation is shown in Figure 7. As the magnetic field intensity increases (when both and are each equal to 1), the trend demonstrates a deteriorating outcome on the velocity (particularly the maximum velocity), which is expected because the Lorentz force in the magnetic field affects the fluid motion.

Figures 8-12 illustrate the variations of heat source/sink on the heat transfer amount and on the frictional force against chemical reacting parameter. Figure 8a and b showcase the function of heat source on the rate of heat transfer. It is demonstrated that growing levels of heat generation speed up the fluid motion at y=0 as shown in figure 8a, while an opposite case is recorded at the wall (y=1) as depicted in figure 8b.

The pattern of heat sink on the heat transfer rate is showcased in figures 9a and b. It is clear from these figures that at the heated wall (y=0), the rate of heat transfer grows while a counter effect is recorded at the micro-channel wall (y=1).

Figures 10a and b display the impact of heat source on the sheer stress. It is worth noting that increasing levels of S contributes to a significant rise in the frictional force at the heated superhydrophobic wall as depicted in figure 9a, whereas the reverse case is recorded at y = 1. Figures 11a and b plot the deviations of heat sink parameter on the skin friction against the chemical reactant parameter. As shown in these graphs, increasing the heat emission parameter increases the drag force at y = 0, while decreasing it at y = 1.
The behavior of the drag force with the variations of mixed convection parameter is depicted in figure 12. It is evident that at the both microchannel walls, a similar downward trend is noticed for growing values of Gre.
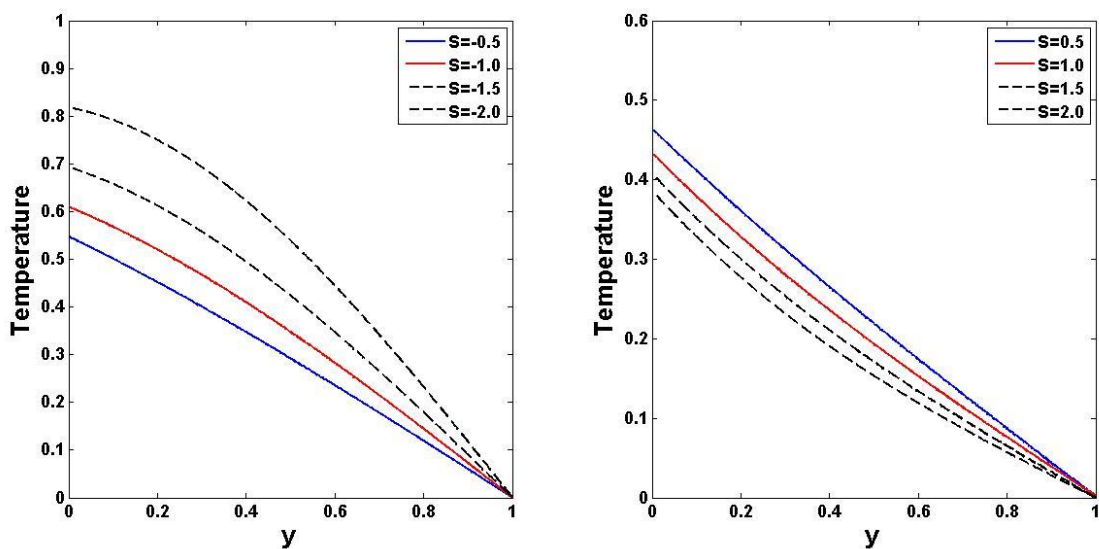
Figure 2: Deviation of temperature for (a) heat generation and (b) heat absorption for constant values of $\gamma = \Gamma = 1$, Ha=0.5, λ =0.001
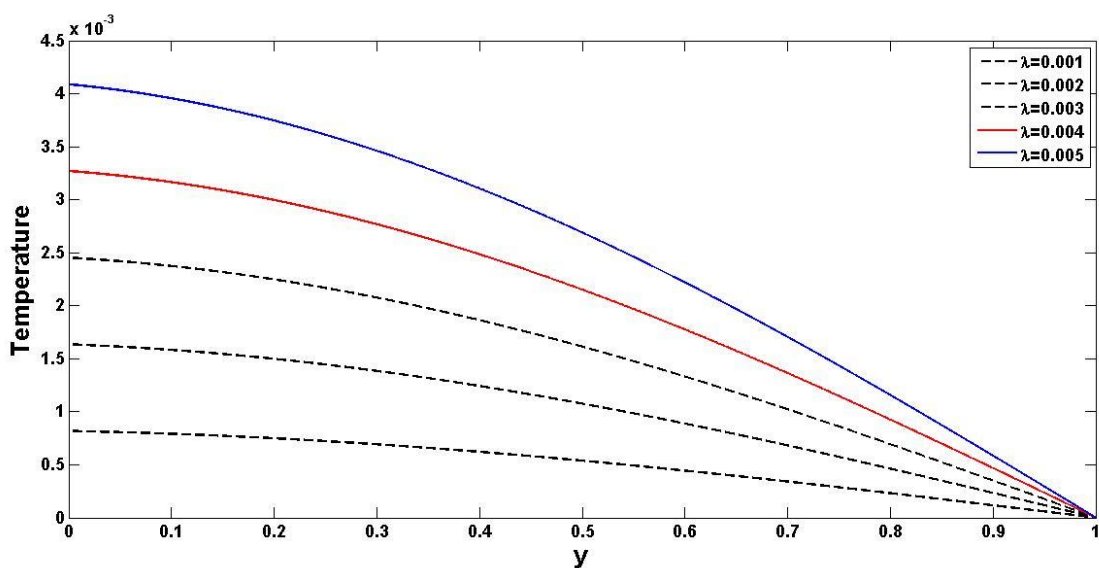

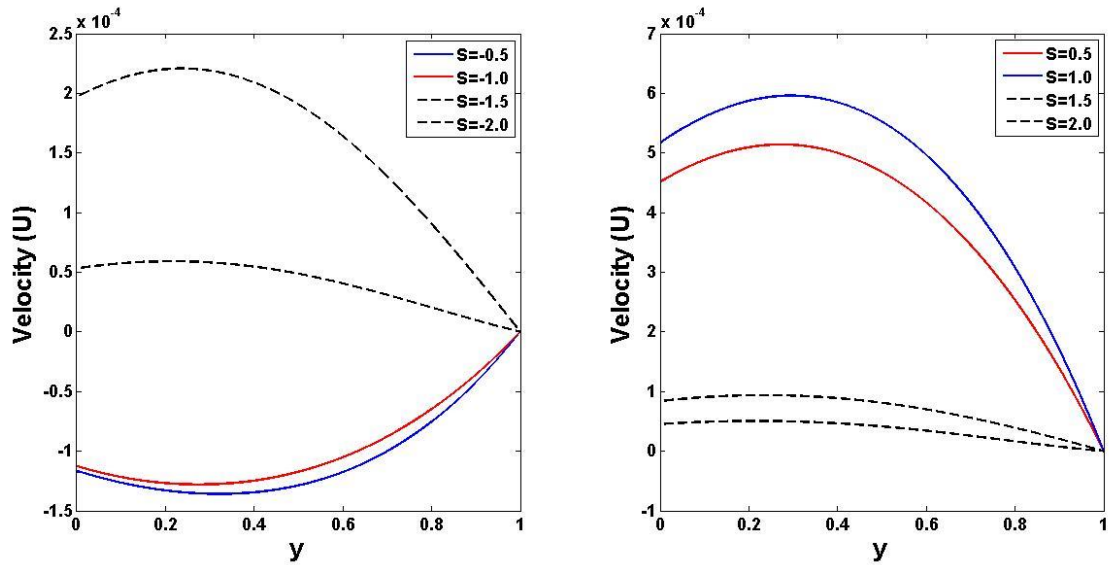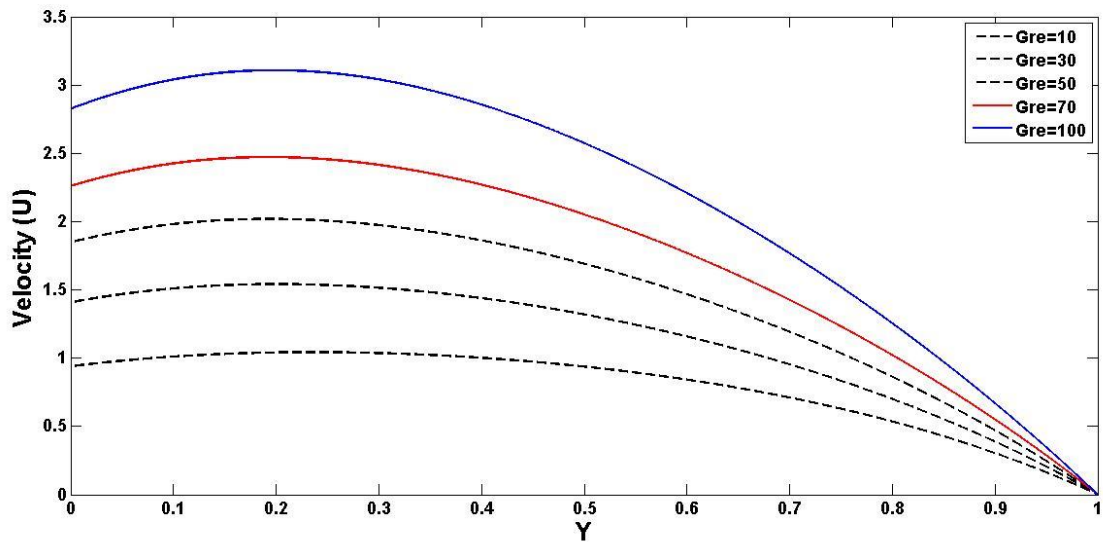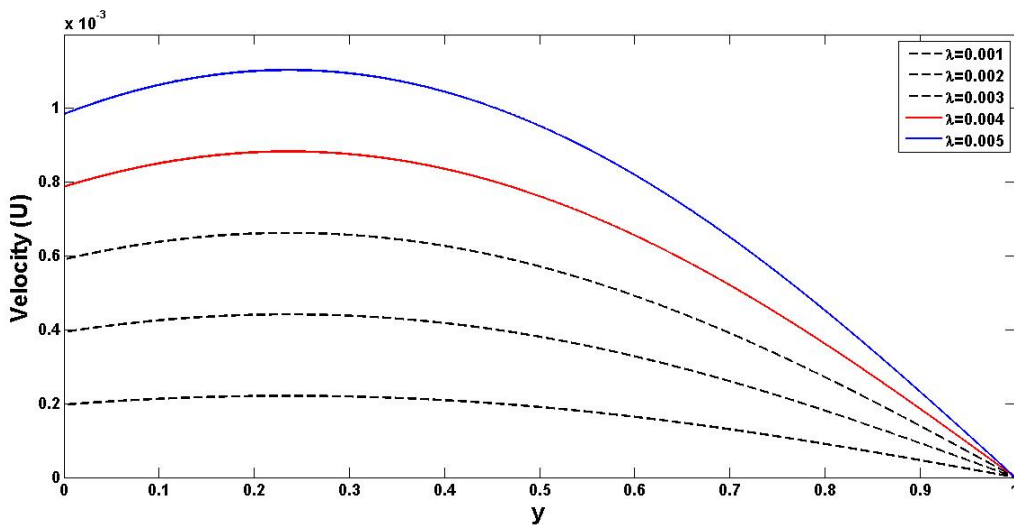Figure 3: Deviation of temperature for λ for constant values of $\gamma = \Gamma = 1$, Ha=0.5, S=-0.5

Figure 4: Deviation of velocity for (a) heat generation and (b) heat absorption for constant values of γ = Γ= 1, Ha=0.5, λ =0.001

Figure 5: Deviation of velocity for mixed convection for constant values of γ = Γ= 1, Ha=0.5, S=-0.5

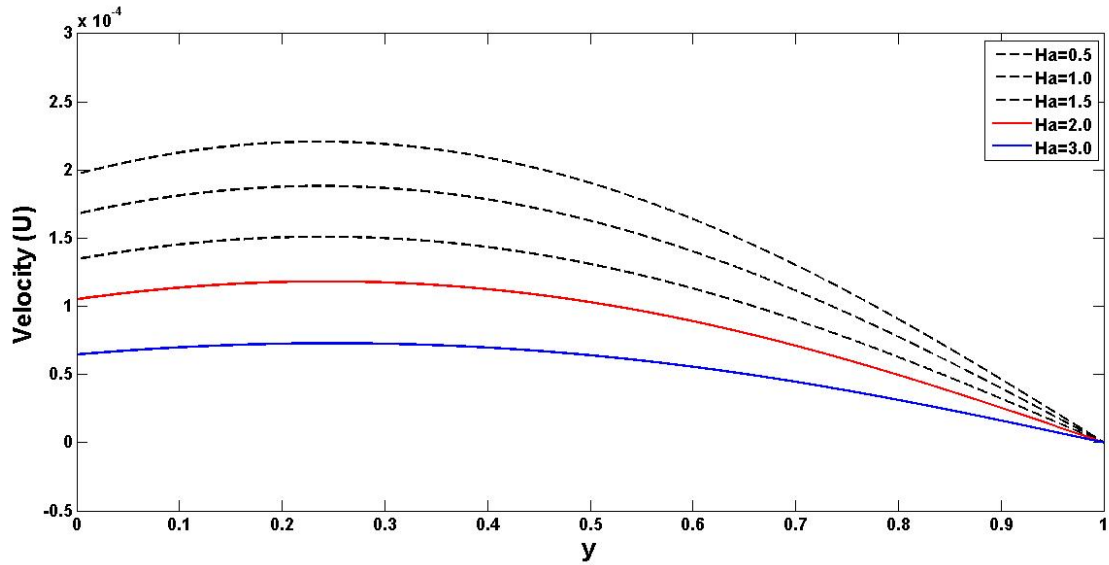Figure 6: Deviation of velocity for λ for constant values of γ = Γ= 1, Ha=0.5, S=-0.5

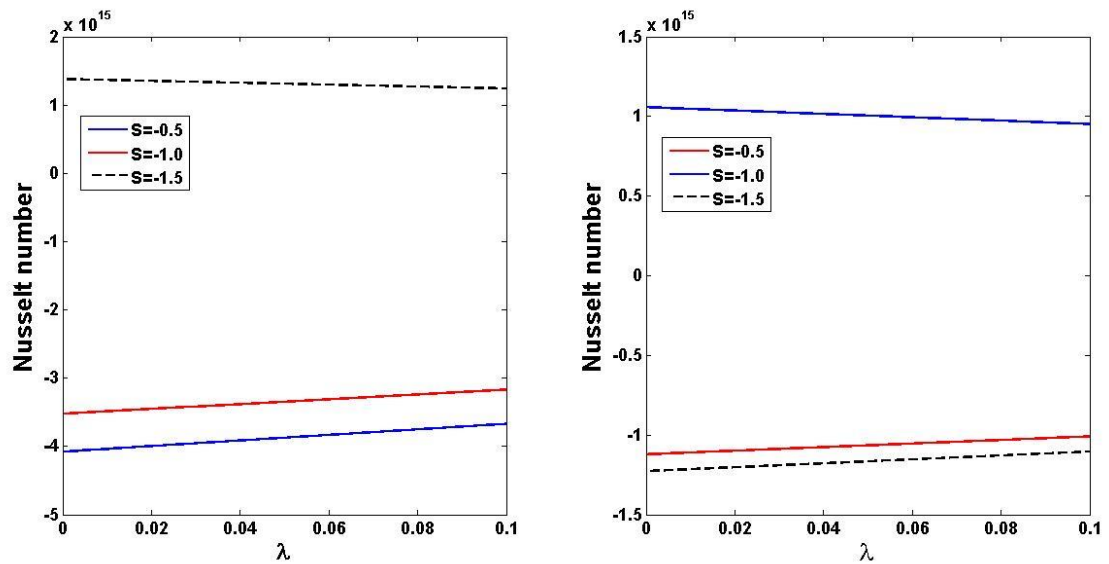Figure 7: Deviation of velocity for MHD for constant values of γ = Γ= 1, λ =0.001, S=-0.5

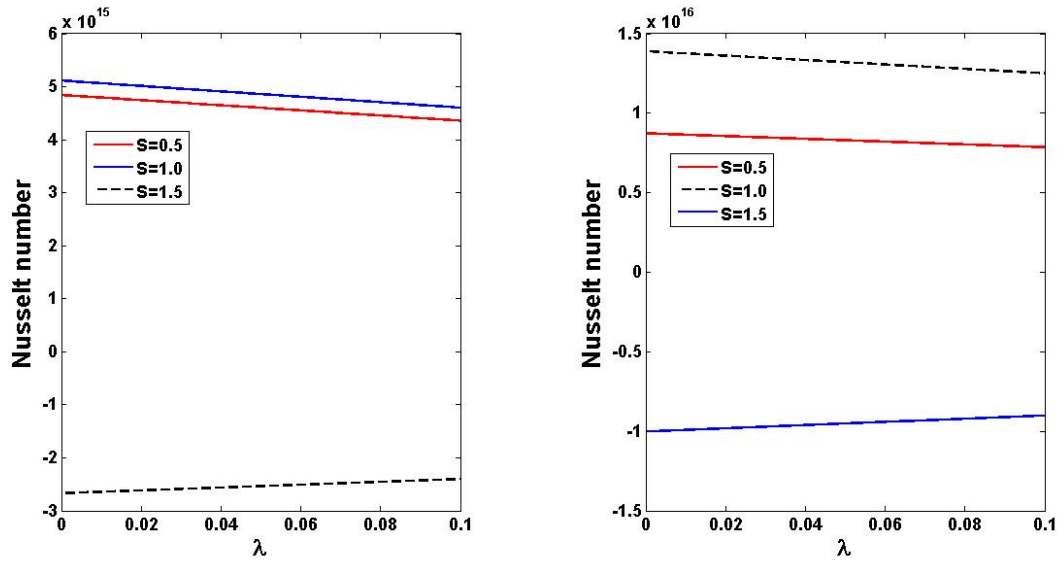Figure 8: Variation for Nusselt number for heat generation at (a) y =0 and (b) y=1 for constant values of γ = Γ= 1,
Ha=0.5

Figure 9: Variation for Nusselt number for heat absorption at (a) y =0 and (b) y=1 for constant values of γ = Γ= 1, Ha=0.5
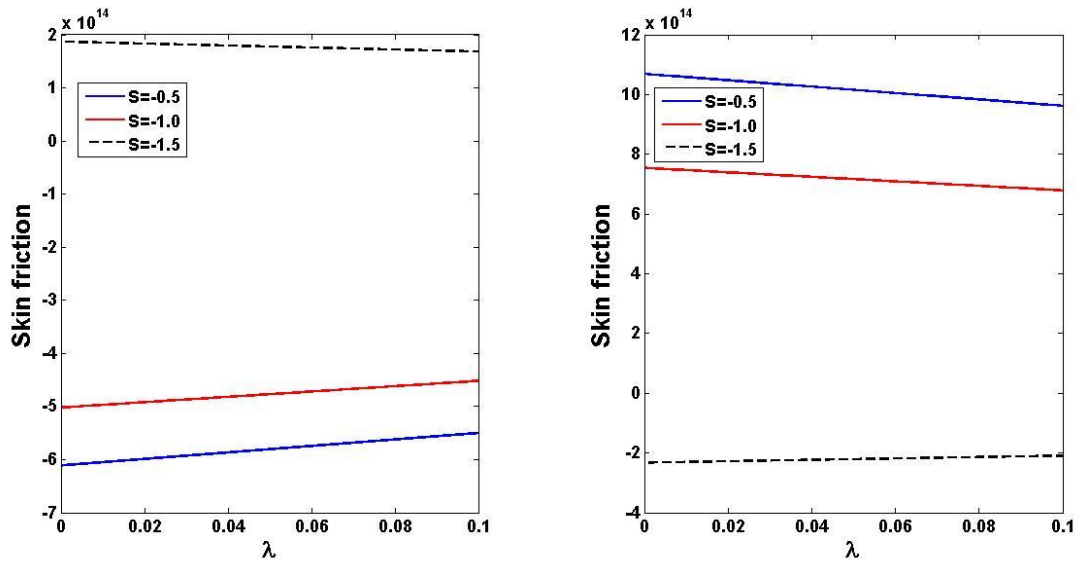

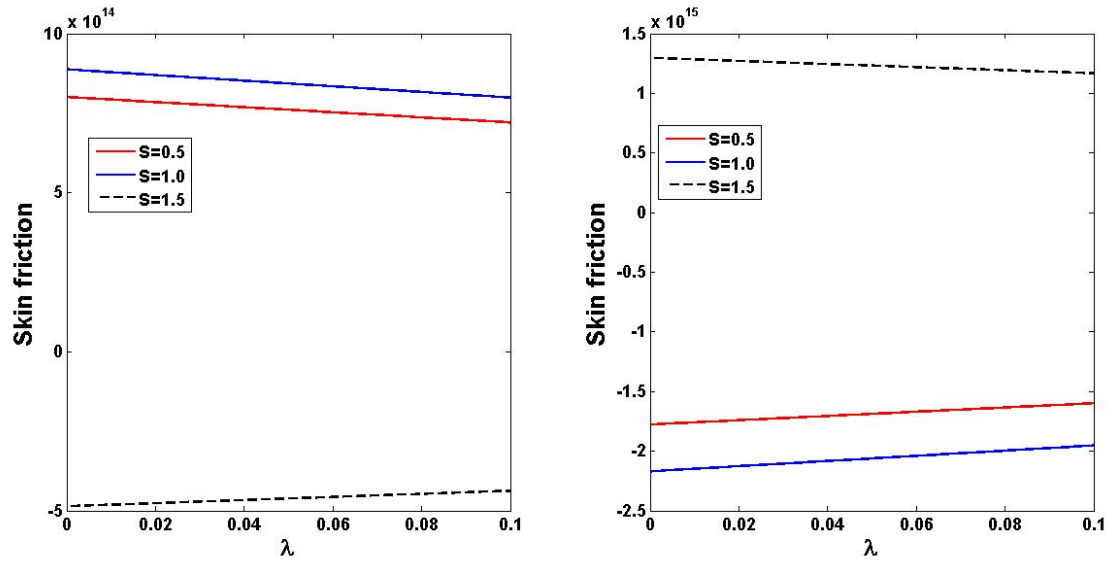Figure 10: Variation for skin friction for heat generation at (a) y =0 and (b) y=1 for constant values of γ = Γ= 1, Ha=0.5

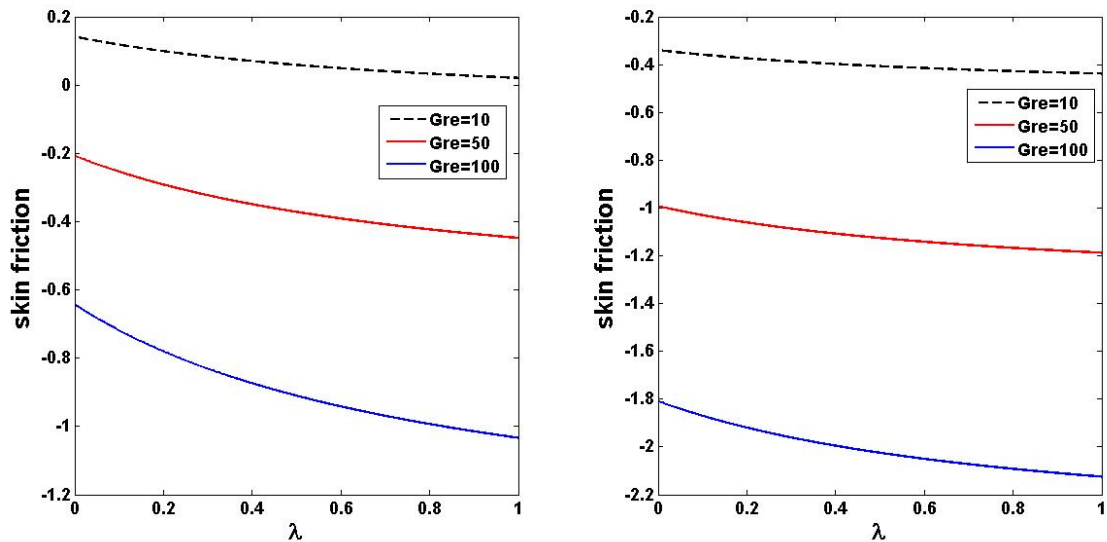Figure 11: Variation for skin friction for heat absorption at (a) y =0 and (b) y=1 for constant values of γ = Γ= 1, Ha=0.5

Figure 12: Variation for skin friction for mixed convection at (a) y =0 and (b) y=1 for constant values of γ = Γ= 1, Ha=0.5

Table 1: Comparison of Jha and Gwandu's (2017) work with the current investigation for velocity and temperature distributions for γ = Γ= 1, Gre=1, Ha = 0.5 when λ and S approaches 0 respectively.

	Jha and Gwandu (2017)		Current work	
	θ (Y)	U(Y)	θ(Y)	U(Y)
Y				
0.1	0.4500	0.0843	0.4498	0.0843
0.2	0.4000	0.0856	0.4000	0.0856
0.3	0.3500	0.0831	0.3500	0.0831
0.4	0.3000	0.0772	0.2998	0.0772
0.5	0.2500	0.0686	0.2499	0.0686

Conclusion

The paper investigated the implications of chemically reacting fluid on the steady mixed convection of an electrically conducting fluid traveling upwardly within an isothermally heated parallel plate in the micro-channel due to heat generation/absorption, with one surface exhibiting super-hydrophobic slip and temperature jump and the other not. The perturbation series approach (semi-analytical method) is applied to address the steady state system of equations, and several illustrated graphs demonstrating the functions of relevant parameters on flow patterns are shown. Comprehending the behavior of these kinds of fluids is particularly significant in both engineering and medicine. The following is a summary of the key findings from this study:

i. The fluid motion and energy distributions are seen to deteriorate significantly when $S > 0$, which suggests heat absorption. However, when $S < 0$, which indicates heat generation, a counter attribute happens.

ii. It was revealed that a surge in the fluid acceleration and thermal distribution is evident as the chemical reactant parameter is mounting

iii. Raising the mixed convection factor promotes the intensity of the fluid flow in the microchannel

iv. Uplifting the chemical reaction parameter, the local frictional force goes down at $y = 0$ and rises at the wall ($y = 1$). Further, a similar trend is noticed on the rate of heat transfer for the same consequence.

v. Increasing the heat source parameter profoundly improves the skin friction and the Nusselt number respectively at the heated micro-channel wall ($y=0$), whereas a counter phenomenon is recorded at $y=1$. However, converse effects are all observed for rising levels of heat sink parameter.

References

Al-Nimr, M. A. and Khadrawi, A. F., (2004). Thermal behavior of a stagnant gas confined in a horizontal microchannel as described by the dual-phase-lag heat conduction model. *International Journal of Thermo-physics*, 25(2),1953–1964

Buonomo, B. and Manca, O., (2012). Natural Convection Flow in a Vertical Micro-Channel with Heated at Uniform Heat Flux, *International Journal of Thermal Sciences*. **49,** 1333-1344.

Chen, C. K. and Weng, H. C., (2005). Natural convection in a vertical micro-channel, *Journal of Heat Transfer,* **127**, 1053-1056.

Geethan, S. K., Kiran, R. K., Vinod, G. K. and Varma, S. V. K., (2016). Soret and Radiation Effects on MHD Free Convection Slip Flow over an Inclined Porous Plate with Heat and Mass Flux, *Advances in Scientific Engineering and Medicine*, **8**(3), pp. 1-10.

Hamza, M. M. Ojemeri G. and Ahmad, S. K., (2023). Theoretical study of Arrhenius-controlled heat transfer flow on natural convection affected by an induced magnetic field in a microchannel, *Engineering Reports, Wiley*, DOI:10.1002/eng2.12642

Hamza, M. M., (2016). Free convection slip flow of an exothermic fluid in a convectively heated vertical channel, *Ain Shams Engineering Journal*, http://dx.doi.org/10.1016/j.asej.2016.08.011

Hatte, S., and Pitchumani, R., (2021). Analysis of convection heat transfer on multiscale rough super-hydrophobic and liquid infused surfaces, 1-29. https://www.sciencedirect.com/science/article/am/pii/S13858947210184

Jha B. K. Aina, B. and Ajiya, A. T., (2014a). MHD natural convection flow in a vertical parallel plate microchannel," Ain shams Eng. J., **6**, pp. 289-295.

Jha B. K. and Aina B., (2016). Role of induced magnetic field on MHD natural convection flow in vertical microchannel formed by two electrically non-conducting infinite vertical parallel plates, *Alexandria Engineering Journal*, **55**(2), 2087-2097.

Jha, B. K., Aina, B. and Isa, S., (2015). Fully developed MHD natural convection flow in a vertical annular micro channel: an exact solution, *Journal of king Saudi University-Sciences*, **27**, pp. 253-259.

Jha, B. K. and Gwandu, B. J., (2019). MHD free convection flow in a vertical slit micro-channel with super-hydrophobic slip and temperature jump: non-linear Boussinesq approximation approach, *SN Applied Sciences*, DOI: 10.1007/S42452-019-0617-Y.

Jha, B. K., Aina B. and Joseph, S. B., (2014b). Natural Convection Flow in vertical Micro-channel with Suction/Injection, *Journal of Proceedings of Mechanical Engineering*, **228**(3), 171-180.

Jha, B. K. and Gwandu, B. J., (2017). MHD free convection flow in a vertical slit micro-channel with super-hydrophobic slip and temperature jump: Heating by constant wall temperature, *Alexandria Engineering Journal*, **57**(3), 2541-2549.

Jha, B. K. and Gwandu, B. J., (2020). MHD free convection flow in a vertical porous super-hydrophobic microchannel, *Journal of Mechanical Engineering*, **235**(2), 1-9.

Jha, B. K. and Malgwi, P. B., (2019a). Hall current and ion – slip effects on free convection flow in a vertical microchannel with induced magnetic field, *Heat Transfer in Asian Research* **48**(8), 1 – 19.

Jha, B. K., Malgwi P. B. and Aina, B., (2017). Hall effects on MHD natural convection flow in a vertical microchannel, *Alexandria Engineering Journal*, http://dx.doi.org/10.1016/j.aej.2017.01.038

Joseph, K. M., Ayuba, P., Nyitor, L. N. and Muhammed, S.M., (2015). Effect of Heat and Mass Transfer on Unsteady MHD Poiseuille flow between Two Infinite Parallel Porous plates in an Inclined Magnetic Field, *International Journal of Scientific Engineering and Applied Sciences*, **1**(5).

Ojemeri G., Omokhuale E., Hamza M. M., Onwubuya I. O. and Shuaibu A., (2023). A Computational Analysis on Steady MHD Casson Fluid Flow Across a Vertical Porous Channel Affected by Thermal Radiation Effect. *International Journal of Science for Global Sustainability*, 9(1), https://doi.org/ 10.57233/ijsgs.v9i1.393

Ojemeri, G. and Hamza, M. M., (2022). Heat transfer analysis of arrhenius-controlled free convective hydromagnetic flow with heat generation/absorption effect in a micro-channel, *Alexandria Engineering Journal*, **61**, pp. 12797-12811.

Ramanuja, M., Krishna, G. G., Sree, H. K. and Radhika, V. N., (2020). Free convection in a vertical slit microchannel with super-hydrophobic slip and temperature jump conditions, *International Journal of Heat Technology*, **38**(3), pp. 738-744.

Sivaiah, G. and Reddy, K. J., (2017). Unsteady MHD heat and mass transfer flow of a radiating fluid past an accelerated inclined porous plate with Hall current, *International Research-Granthaalayah*, **5**(7), 42-59.

Siva, T., Jaangili, S. and Kumbhakar, B., (2021). Heat transfer analysis of MHD and electroosmotic flow of non-Newtonian fluid in a rotating microfluidic channel: an exact solution, *Applied Mathematics and Mechanics*, **42**, 1047-1062.

Taid, B. K. and Ahmed, N. B., (2022). MHD free convection flow across an inclined porous plate in the presence of heat source, Soret effect and chemical reaction affected by viscous dissipation ohmic heating, *Bio-interface Research in Applied Chemistry*, **12**(5), 6280-6296.

Weng, H. C. and Chen, C. K., (2009). Drag reduction and heat transfer enhancement over a heated wall of a vertical annular microchannel, *International Journal of Heat and Mass Transfer*, **52,** 1075–1079.